PLANT SCIENCES

Natural variation of codon repeats in *COLD11* endows rice with chilling resilience

Zhitao Li[1,2]†, Bo Wang[1,2]†, Wei Luo[1,2], Yunyuan Xu[1,2], Jinjuan Wang[3], Zhihui Xue[1], Yuda Niu[1], Zhukuan Cheng[4,5], Song Ge[2,6], Wei Zhang[7], Jingyu Zhang[1,2]*, Qizhai Li[2,7]*, Kang Chong[1,2]*

Abnormal temperature caused by global climate change threatens the rice production. Defense signaling network for chilling has been uncovered in plants. However, less is known about repairing DNA damage produced from overwhelmed defense and its evolution during domestication. Here, we genetically identified a major QTL, *COLD11*, using the data-merging genome-wide association study based on an algorithm combining polarized data from two subspecies, *indica* and *japonica*, into one system. Rice loss-of-function mutations of *COLD11* caused reduced chilling tolerance. Genome evolution analysis of representative rice germplasms suggested that numbers of GCG sequence repeats in the first exon of *COLD11* were subjected to strong domestication selection during the northern expansion of rice planting. The repeat numbers affected the biochemical activity of DNA repair protein COLD11/RAD51A1 in renovating DNA damage under chilling stress. Our findings highlight a potential way to finely manipulate key genes in rice genome and effectively improve chilling tolerance through molecular designing.

INTRODUCTION

In recent years, the cultivation of rice, one of the most important food crops feeding nearly half of the world's population, has been threatened by abnormal environmental temperatures (such as chilling) induced by global climate change (*1*, *2*). The bottleneck limiting rice-planting region expansion to northern areas with much lower yearly temperatures is the improvement of chilling tolerance for rice cultivars, because rice is sensitive to chilling and the ability to tolerate low temperature is pivotal for its survival. The two subspecies of Asian cultivated rice (*Oryza sativa*), *japonica* (*O. sativa* ssp. *japonica*) and *indica* (*O. sativa* ssp. *indica*), have different abilities to tolerate chilling stress. *Japonica*, with stronger chilling tolerance, predominates in temperate and some subtropical zones, while *indica*, sensitive to chilling, grows mainly in tropical/subtropical regions. Chilling tolerance is a complex trait genetically controlled by several key quantitative trait loci (QTLs) (*3*–*5*). These genetic loci and their major genes may be used as molecular modules to improve the tolerance of rice cultivars to low environmental temperature (*6*). So far, some QTLs, such as *COLD1* and *CTB4a*, have been identified to contribute to chilling tolerance (*7*, *8*). The sensor complex chilling tolerance divergence 1 (COLD1)/G-protein α subunit 1 (RGA1) triggers calcium signaling and activates downstream factors, such as OsMAPK3, OsbHLH002, and OsTPP1, which mediate subsequent responses to prevent chilling damage and developmental adjustment (*7*, *9*, *10*). On the other hand, DNA damage still occurs during chilling stress, which breaks the defense line. Its regulation mechanism, however, is largely unknown. There is a need to obtain a comprehensive understanding of the regulation mechanisms for all cases to be used in rice molecular design breeding to improve agricultural production.

RESULTS

More QTLs are identified by data-merging GWAS

Because of the polarization of *japonica* and *indica* in chilling tolerance, it is not easy to include them in the same analyzing system using reported algorithms in a genome-wide association study (GWAS). No obvious phenotypic changes are observed for seedlings of *japonica* with mild-level chilling treatment, while all the *indica* seedlings die under severe treatment, which makes it almost impossible to perform GWAS for both *japonica* and *indica* in one analytic system.

In this study, we used an alternative mathematic approach with multidimensional scaling (MDS) to integrate the chilling tolerance data from both *japonica* (292 accessions) and *indica* (172 accessions) for GWAS, named as data-merging GWAS. The approach using merged phenotypic data identified QTLs contributing to rice chilling tolerance, especially those specific for *japonica*. After data combination, the total number of individuals was 464, almost twice as many as in the *japonica* dataset. Through genome resequencing, 5,108,184 single-nucleotide polymorphisms (SNPs) were genotyped. After excluding the SNPs with missing rates larger than 20%, a minimal count of three genotypes less than 5, and minor allele frequency less than 5%, 2,134,700 SNPs passed the quality control step and were retained for further analysis.

Because of the different cold tolerance of *japonica* and *indica*, it was measured with two durations of chilling treatment, 30 and 60 hours, the former of which was applicable to *indica* and the latter of which was appropriate for *japonica*. MDS approach was

[1]Key Laboratory of Plant Molecular Physiology, Institute of Botany, Chinese Academy of Sciences, Beijing 100093, China. [2]University of Chinese Academy of Sciences, Beijing 100049, China. [3]School of Mathematics and Statistics, Beijing Institute of Technology, Beijing, 100181, China. [4]State Key Laboratory of Plant Genomics, Institute of Genetics and Developmental Biology, Chinese Academy of Sciences, Beijing 100101, China. [5]Jiangsu Co-Innovation Center for Modern Production Technology of Grain Crops, Yangzhou University, Yangzhou 225009, China. [6]State Key Laboratory of Systematic and Evolutionary Botany, Institute of Botany, Chinese Academy of Sciences, Beijing 100093, China. [7]LSC, NCMIS, Academy of Mathematics and Systems Science, Chinese Academy of Sciences, Beijing 100190, China.
†These authors contributed equally to this work.
*Corresponding author. Email: chongk@ibcas.ac.cn (K.C.); liqz@amss.ac.cn (Q.L.); jingyuzhang@ibcas.ac.cn (J.Z.)

used to combine these two datasets while preserving interpoint variation (Fig. 1A and Materials and Methods).

We assessed the evidence of association using the Bayes factor (BF) (*11*), which is the ratio of the probability of observed data under the alternative hypothesis of a true association to that under the null hypothesis. The advantage for BF is that its strength of evidence does not vary with factors that affect power, such as sample size and minor allele frequency (*12*). As a comparison,

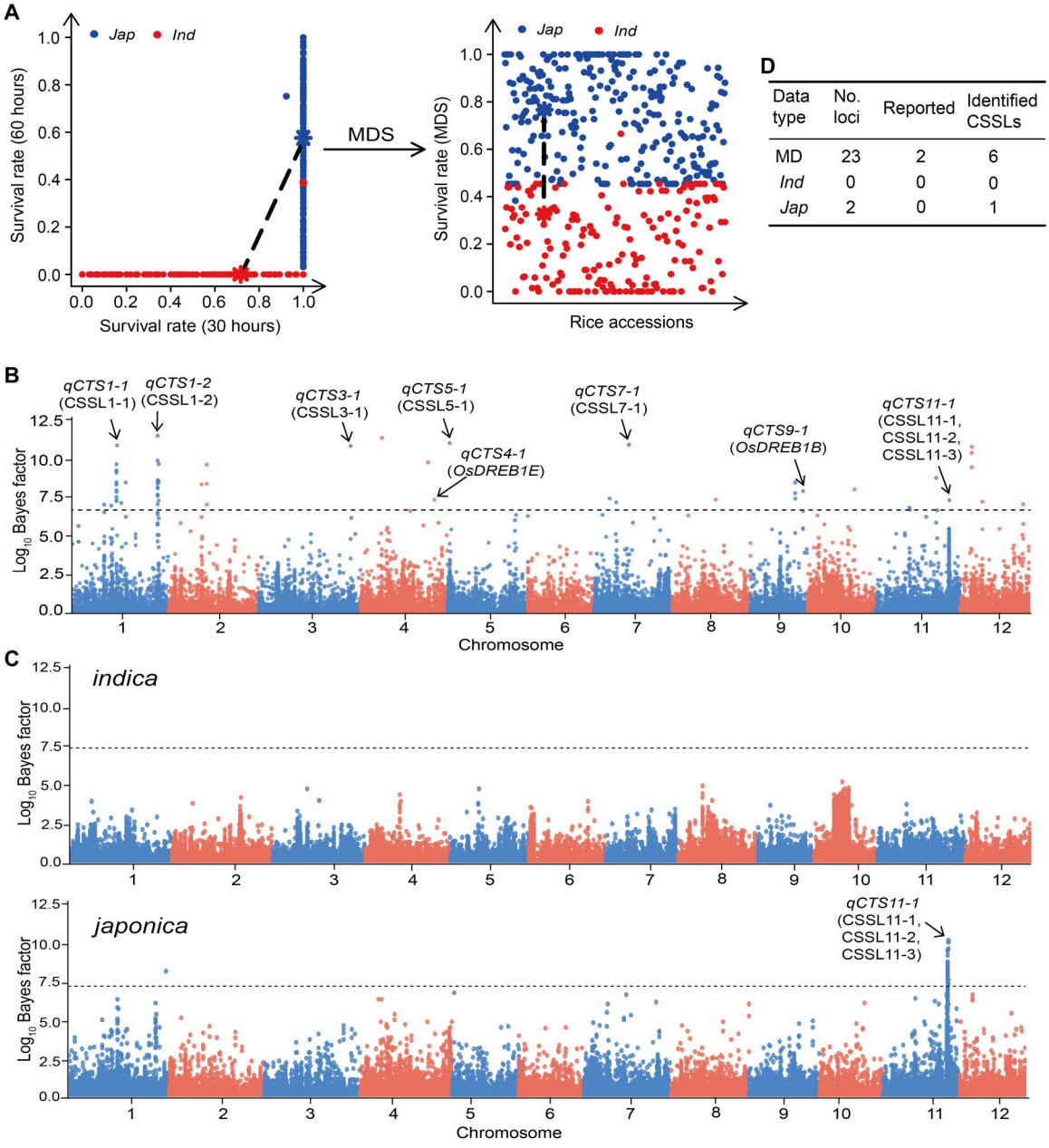

D

Data type	No. loci	Reported	Identified CSSLs
MD	23	2	6
Ind	0	0	0
Jap	2	0	1

Fig. 1. Data-merging GWAS for rice chilling tolerance with separate analysis for *indica* and *japonica* as control. (**A**) Schematic diagram showing the merging of survival rate data for *indica* and *japonica*. Blue and red stars stand for random samples in *japonica* (*Jap*) and *indica* (*Ind*), respectively. The line connecting these two stars stands for interpoint distance, which is preserved before and after data merging. (**B**) Manhattan plots of the Bayes factor result of data-merging GWAS for chilling tolerance. Horizontal axis indicates chromosomes, and vertical axis indicates $\log_{10}$ (Bayes factor). Dashed line represents significance threshold ($\log_{10}$ BF = 6.77). Arrows indicate the positions of strong peaks (*qCTS1-1*, *qCTS1-2*, *qCTS3-1*, *qCTS4-1*, *qCTS5-1*, *qCTS7-1*, *qCTS9-1*, and *qCTS11-1*), which were confirmed by chilling tolerance analysis of chromosome segment substitution lines (CSSLs; CSSL1-1, CSSL1-2, CSSL3-1, CSSL5-1, CSSL7-1, CSSL11-1, CSSL11-2, and CSSL11-3) or contained reported chilling tolerance–related genes (*OsDREB1B* for *qCTS9-1* and *OsDREB1E* for *qCTS4-1*). (**C**) Manhattan plots of the Bayes factor results of GWAS for chilling tolerance of *indica* (top) and *japonica* (bottom). Dashed line represents significance threshold (*indica*: $\log_{10}$ BF = 7.32 and *japonica*: $\log_{10}$ BF = 7.32). Arrow indicates the position of strong peak, *qCTS11-1*, which was confirmed by analysis of CSSL11-1, CSSL11-2, and CSSL11-3. (**D**) Statistical data for data-merging GWAS and GWAS performed separately for *indica* and *japonica*. MD, merged data; *Ind*, *indica* data; *Jap*, *japonica* data; No. loci, number of loci exceeding significance threshold; Reported, the number of loci with chilling tolerance–related genes reported previously; Identified CSSLs, the number of loci confirmed by CSSLs.

GWAS analysis was also performed with *indica* and *japonica* separately, with only a few signals notably associated with traits being identified (Fig. 1C). However, a number of significant loci were identified with GWAS using merged phenotypic data, and the SNPs that exceeded the significance threshold were ranked from largest to smallest (Fig. 1, B and D, and dataset S1). Among the higher-ranked SNPs, eight of them, with high-association loci, could be confirmed by either previous research or cold tolerance analysis of chromosome segment substitution lines (CSSLs; a series of high-generation backcross lines obtained by backcrossing first filial generation (F_1) with recurrent parents for multiple generations and every one of them carries one or more donor chromosome segments in the genetic background of the recipient) (Figs. 1, B and D, and 2A and fig. S1, A and B) (*13*–*15*). Genes previously reported to contribute to chilling tolerance, *OsDREB1E* and *OsDREB1B*, are located within *qCTS4-1* and *qCTS9-1*, respectively (*13*, *14*). *OsDREB1E* is only 20 kb from the highest peak of *qCTS4-1*. Five QTLs—*qCTS1-1*, *qCTS1-2*, *qCTS3-1*, *qCTS5-1*, and *qCTS7-1*—were confirmed by chilling tolerance analysis of CSSLs CSSL1-1, CSSL1-2, CSSL3-1, CSSL5-1, and CSSL7-1, respectively, which contain Nipponbare (NIP; *japonica*) chromosome introgressions carrying corresponding QTLs in 93-11 (*indica*) background (Fig. 2, A and B, and fig. S1, A and B) (*15*). The QTL *qCTS11-1* was confirmed by analysis of three CSSLs: CSSL11-1, CSSL11-2, and CSSL11-3 (Fig. 2, A and B, and fig. S1A). CSSL11-1 and CSSL11-3 contained a W1943 (*Oryza rufipogon* Griff.) and NIP (*japonica*) genomic introgression carrying the *qCTS11-1* in Guangluai 4 (GLA4; *indica*) background, respectively. CSSL11-2 carried a Suyunuo (SYN; *indica*) substitution segment corresponding to the *qCTS11-1* region in Huajingxian 74 (HJX74; *indica*) background (fig. S1A). In chilling tolerance analysis, the lines CSSL1-1, CSSL1-2, CSSL3-1, CSSL5-1, CSSL7-1, CSSL11-1, and CSSL11-3 exhibited higher chilling tolerance than wild type. On the contrary, CSSL11-2 exhibited lower chilling tolerance compared with wild type (Fig. 2, A and B). Explanation is provided afterward. To further determine whether the phenotypes of CSSLs have connection with known genes, such as *OsICE1*, *OsDREB1A*, *OsDREB1B*, and *OsDREB1C*, their expression patterns were monitored (fig. S1, C to F) (*9*, *13*). The expression levels of *OsICE1* in CSSL3-1 and CSSL7-1 were much higher than that in wild-type control 93-11, suggesting that they were related to the ICE1/OsbHLH002-CBF/OsTPP1 pathway (fig. S1C).

These results demonstrate that our data-merging method is an effective approach and could be applicable for the combination of

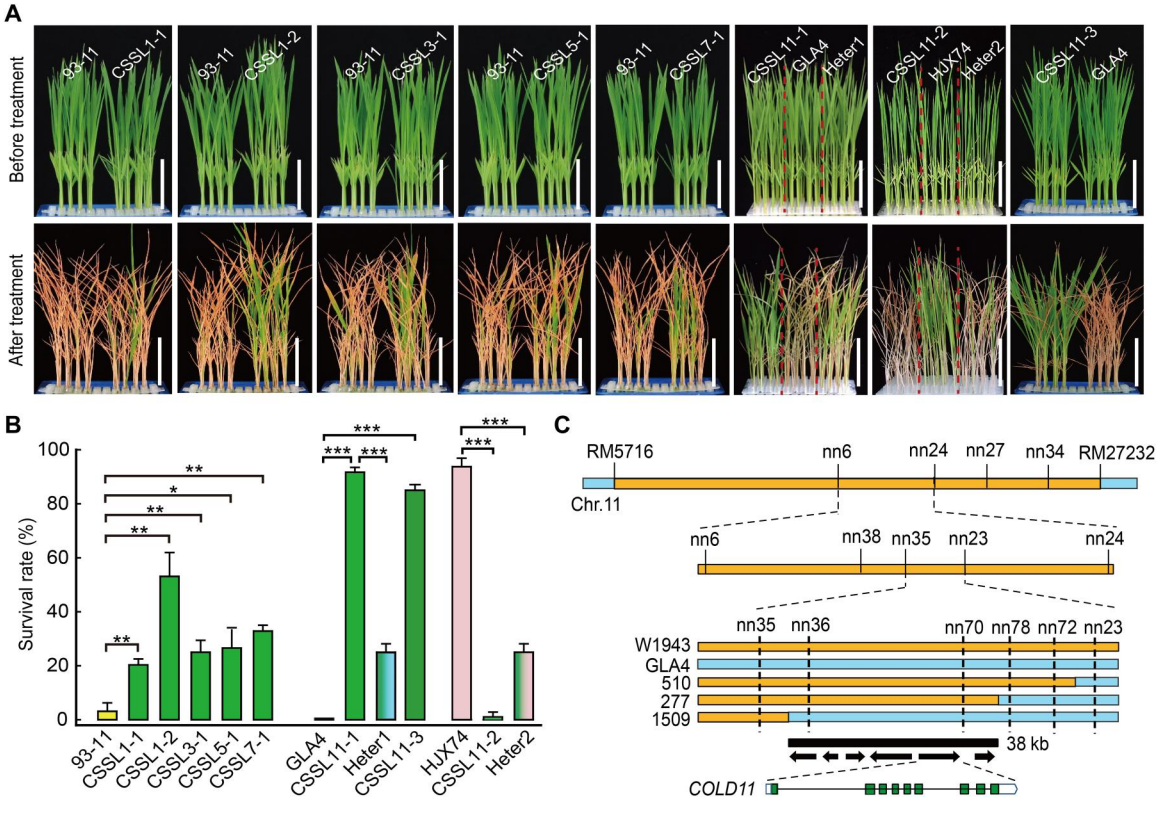

Fig. 2. Confirmation of GWAS results with CSSLs and map-based cloning of *COLD11*. (**A**) Phenotypic response to chilling for the CSSLs CSSL1-1, CSSL1-2, CSSL3-1, CSSL5-1, CSSL7-1, CSSL11-1, CSSL11-2, and CSSL11-3; the recurrent parents 93-11, GLA4, and HJX74; and the heterozygotes Heter1 for CSSL11-1 and Heter2 for CSSL11-2. Scale bars, 5 cm. (**B**) Survival rates for plant materials in (A). Values are shown as means ± SD ($n = 3$). P values were generated using Student's t test; $^*P < 0.05$, $^{**}P < 0.01$, and $^{***}P < 0.001$. (**C**) Fine mapping of *COLD11* using BC_7F_2 plants derived from the backcross of CSSL11-1 with GLA4 narrowed to a 38-kb genomic region containing six predicted genes: *LOC_Os11g40110*, *LOC_Os11g40120*, *LOC_Os11g40130*, *LOC_Os11g40140*, *LOC_Os11g40150*, and *LOC_Os11g40160*. Light blue and saffron yellow rectangles represent GLA4 and W1943 genomic regions, respectively. The characters upon saffron yellow rectangles are molecular makers. Black rectangles represent the fine-mapped 38-kb genomic region, black arrows represent predicted genes, and green rectangles represent exons of *COLD11*. Individual plants 510, 277, and 1509 were selected from the mapping population and used for fine mapping.

divergent data. *qCTS11-1*, which could be confirmed by three different CSSLs, was chosen for further analysis (Fig. 2, A and B).

COLD11 confers chilling tolerance in rice

To identify the major gene underlying *qCTS11-1*, two mapping populations were generated using corresponding CSSLs (CSSL11-1 and CSSL11-2) with obvious change in chilling tolerance. Fine-scale mapping of *qCTS11-1* using 11,000 BC_7F_2 plants derived from the backcross of GLA4 with CSSL11-1 and 3000 BC_7F_2 plants derived from the backcross of HJX74 with CSSL11-2 narrowed the candidate region to a 38-kb segment. This region contains six predicted open reading frames (Fig. 2C; http://rice.plantbiology.msu.edu). No nonsynonymous SNPs were detected in *LOC_Os11g40110*, *LOC_Os11g40120*, *LOC_Os11g40130*, *LOC_Os11g40140*, and *LOC_Os11g40160* simultaneously between W1943 and GLA4, as well as between SYN and HJX74. There were, however, different types of short sequence repeats encoding alanine in the first exon of *LOC_Os11g40150* in W1943, GLA4, HJX74, and SYN (fig. S2A). These data suggested that *LOC_Os11g40150* might be the candidate major gene for *qCTS11-1*, and it was named *CHILLING TOLERANCE DIVERGENCE 11* (*COLD11*).

Genome-edited lines for *COLD11* were generated to confirm its contribution to chilling tolerance. Loss-of-function mutants, *cold11-1* and *cold11-2*, with large fragment deletions in the first exon in GLA4 (*indica*) background, were obtained using the CRISPR-Cas9 system (Fig. 3A and fig. S2, B and C). The mutants exhibited lower tolerance to chilling stress compared with wild type, while the two complementation lines COM^{W1943}*-1* and COM^{W1943}*-2* partially rescued the decreased chilling tolerance phenotype of the frameshift mutant *cold11-1*, which indicates that *COLD11* modulates chilling tolerance in rice and is the functional gene for *qCTS11-1* (Fig. 3, C and D, and fig. S2F). To analyze the biological function of different *COLD11* alleles, two knockout mutants with a large deletion in the second exon, *cold11-3* and *cold11-4*, were also obtained in CSSL11-1 through CRISPR-Cas9–mediated editing (Fig. 3B and fig. S2, D and E). The *cold11-3* and *cold11-4* mutants also showed lower chilling tolerance (survival rates of 11 and 23%, respectively) compared with wild-type control CSSL11-1 (survival rate of 91%) (Fig. 3, C and D), confirming the function of different *COLD11* alleles in chilling tolerance. Furthermore, loss-of-function mutants, *cold11-1* and *cold11-3*, the complementation line COM^{W1943}*-1*, wild-type control GLA4, and CSSL11-1 were stained with FDA/PI (fluorescein diacetate/propidium iodide) to evaluate the number of live/dead cells (*16*). Under normal temperature (25°/28°C, night/day), there was no obvious difference in the number of live/dead cells (fig. S2G). After chilling treatment, however, more dead cells were observed in *cold11-1* than in GLA4 and COM^{W1943}*-1* and also more in *cold11-3* than in CSSL11-1 (Fig. 3, E and F), which is consistent with the results of chilling tolerance analysis (Fig. 3, C and D).

COLD11 was strongly selected during domestication

In genomic sequence analysis, it is notable that there are different types of GCG codon repeats encoding alanine in the first exon of *COLD11* in different rice varieties (dataset S2). To explore the relationship between these repeats and chilling tolerance, we examined the tolerance to chilling stress for *indica*, *temperate japonica*, and *tropical japonica* varieties with different types of GCG repeats. The results showed that rice varieties with three GCG repeats—such as Zhefu 802 (ZF802), GLA4, IR64, and Ai-Chiao-Hong—exhibited lower chilling tolerance compared with varieties with more than three repeats, such as ASU, SALSI, ATH HAGARI JARAHAN PADDY (ATH HAGARI), and DINORADO (Fig. 4 and fig. S3). Note that $COLD11^{W1943}$ contains 10 GCG repeats, and $COLD11^{NIP}$ contains two (TCG + 3GCG) repeats, while $COLD11^{GLA4}$ contains three GCG repeats (fig. S2A). CSSL11-1, in which $COLD11^{GLA4}$ was replaced by $COLD11^{W1943}$, was more tolerant to chilling compared with GLA4 (Fig. 2, A and B, and fig. S2A). CSSL11-3, in which $COLD11^{GLA4}$ was replaced by $COLD11^{NIP}$, was also more tolerant to chilling compared with GLA4 (Fig. 2, A and B, and fig. S2A). Similarly, $COLD11^{HJX74}$ contains four GCG repeats, while $COLD11^{SYN}$ contains three (fig. S2A). Therefore, CSSL11-2, with $COLD11^{SYN}$ substituting for $COLD11^{HJX74}$, was less tolerant to chilling compared with HJX74 (Fig. 2, A and B). These results show that rice varieties with more GCG codon repeats have higher chilling tolerance. To clarify whether other variations in candidate interval, in addition to GCG codon repeats in *COLD11*, also contribute to chilling tolerance, Pearson correlation coefficient analysis was performed between chilling tolerance and all the variations in candidate interval from fine mapping (Fig. 2C) (*17*). As a result, the GCG repeat variation exhibits the highest Pearson correlation coefficient, which is much higher than that for others (fig. S1G), indicating that GCG repeat is the variation responsible for chilling tolerance alteration.

A phylogenetic tree was generated with 43 *indica*, 15 temperate *japonica*, 8 tropical *japonica*, and 4 *Aus* varieties using the *COLD11* genome sequence (*18*). Classification was mainly based on GCG repeat number, with reference to TCG prefix for one type of GCG repeat. All of the temperate *japonica* varieties containing *COLD11* with two (TCG + 3 GCG) repeats were grouped together except for Xindao38, which is a three-line hybrid variety with Zhenshan97 (*indica*) as one of its original parents. Most of the *indica* varieties carried *COLD11* with 3 GCG (Fig. 5A). The distribution of *COLD11* alleles in rice cultivars was also connected with terrestrial temperature. Rice cultivars containing *COLD11* alleles with 3 GCG dominate in tropical zones such as the southern part of China, India, Laos, Cambodia, and Thailand, while the distribution of cultivars carrying *COLD11* alleles with more than three GCG repeats shows northern expansion and exhibits few geographical restrictions, probably due to their higher cold tolerance (Fig. 5B). These results suggest that the role of GCG codon repeats in the evolution of *COLD11* under selection is related to local environmental temperature in rice production.

We also analyzed the nucleotide diversity of different alleles using *COLD11* genome sequence. The values of two measures of diversity (π and θ) for the allele with three GCG repeats (3 GCG) and the allele with two copies of TCG plus three GCG repeats [(TCG + 3 GCG) × 2] were zero and very low, respectively, in contrast to two other alleles, which had relatively higher diversity values (Fig. 5C). These observations suggest that the alleles with 3 GCG and (TCG + 3 GCG) × 2 may have evolved under strong selection, which is consistent with the low and high chilling tolerances of rice cultivars containing these alleles, respectively. In brief, the selection on *COLD11* is related to environment temperature and may contribute to the divergence of rice chilling tolerance.

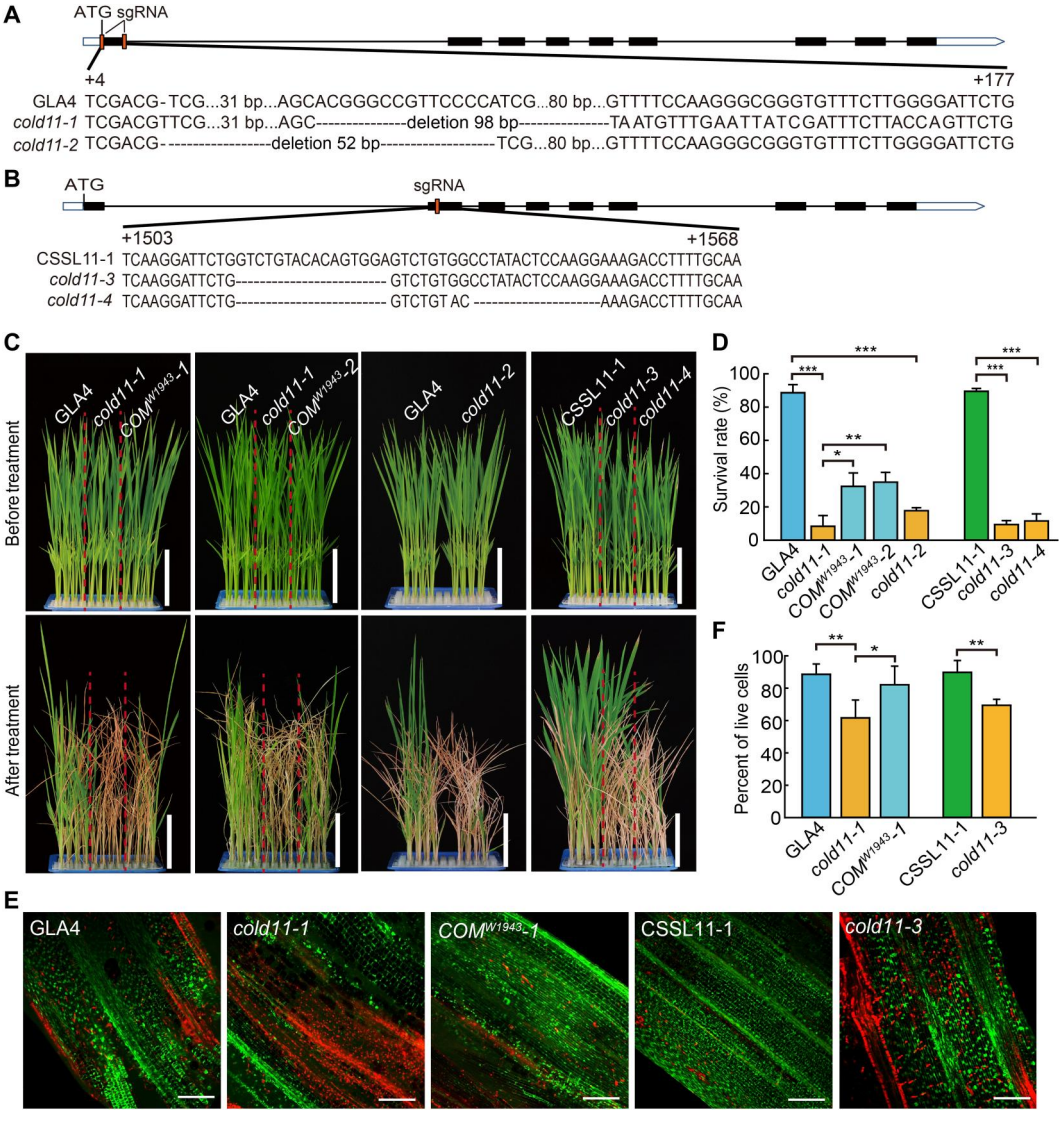

Fig. 3. *COLD11* is required for chilling tolerance. (**A**) Alignment of *COLD11* sequences for *cold11-1*, *cold11-2*, and wild-type GLA4, showing the mutation sites. (**B**) Alignment of *COLD11* sequences for *cold11-3*, *cold11-4*, and wild-type CSSL11-1, showing the mutation sites. Black rectangles in (A) and (B) represent exons of *COLD11*. Numbers with plus sign denote the start and stop position of the indicated region. (**C**) Phenotypic responses to chilling stress for *COLD11* knockout mutants and the complementation line at the seedling stage. *cold11-1* and *cold11-2* are knockout mutants with GLA4 background. COM^{W1943}*-1* and COM^{W1943}*-2* are the complementation line for *cold11-1*. *cold11-3* and *cold11-4* are knockout mutants in the CSSL11-1 background. Scale bars, 5 cm. (**D**) Survival rates for plant materials in (C) after chilling treatment. Values are shown as means ± SD ($n = 3$). (**E**) Fluorescein diacetate/propidium iodide (FDA/PI) staining for live/dead cells after chilling stress in plants in (C). Scale bars, 100 μm. (**F**) Quantification of the percentage of live cells after chilling stress using images corresponding to those in (E). Fluorescence intensity was quantified with the ImageJ plot profile tool (ImageJ v.1.8.0; https://imagej.nih.gov/ij/download.html), and analyses were performed in three biological replicates and shown as means ± SD. *P* values in (D) and (F) were generated using Student's *t* test; $^*P < 0.05$, $^{**}P < 0.01$, and $^{***}P < 0.001$. bp, base pair; sgRNA, single-guide RNA.

COLD11 is responsible for cold-induced double-strand break repair

DNA double-strand breaks (DSBs), generated by various inducing factors, are deleterious genetic lesions that can lead to mutations, rearrangements, or loss of parts of chromosomes. They affect cell metabolism, viability, and even cause cell death (*19*–*23*). *COLD11* is predicted to encode a DNA repair protein, RAD51A1, which plays an essential role in the repair of DNA DSBs by binding to single-stranded DNA (ssDNA) or double-stranded DNA (*24*–*26*). To analyze the biochemical role of *COLD11* in DSB repair in response to chilling, an immunofluorescence assay (IFA) and Western blot analysis were performed using root tips, where *COLD11* is highly expressed, for example, in the *indica* variety GLA4 (fig. S4C). As expected, more severe DSBs were observed in both the *cold11-1* and *cold11-3* mutants compared with wild-type control GLA4 after chilling treatment. In the complementation line COM^{W1943}*-1*, the severe DSB lesion phenotype of *cold11-1* was partially rescued, demonstrating that COLD11 promotes DSB repair during chilling stress (Fig. 6, A and B). Corresponding to the higher chilling tolerance of CSSL11-1, much fewer DSBs were observed in this CSSL compared with wild-type control GLA4, implying the important role of GCG codon repeats in DSB repair

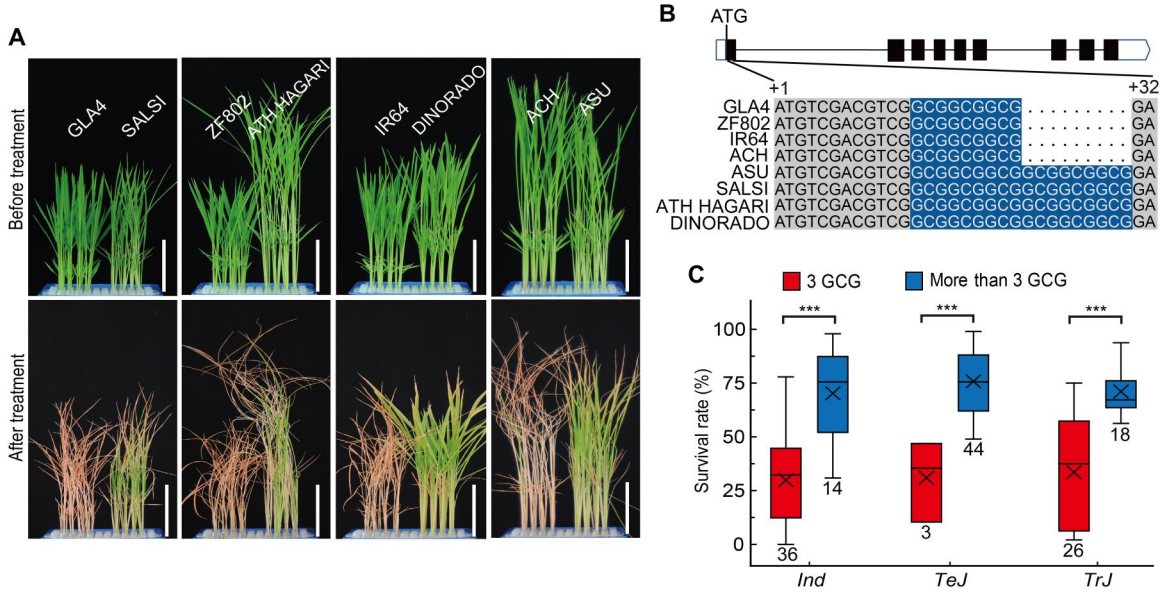

Fig. 4. Cold tolerance conferred by *COLD11* depends on the number of alanine repeats. (**A**) Phenotype of rice cultivars containing *COLD11* with different numbers of GCG repeats, as shown in (B), exposed to chilling at the seedling stage. Scale bars, 5 cm. GLA4, Guangluai 4; ZF802, Zhefu 802; ATH HAGARI, ATH HAGARIJARAHANPADDY; ACH, Ai-Chiao-Hong. (**B**) Different numbers of GCG repeats in the first exon of *COLD11* in the different rice cultivars shown in (A). Diagrams of *COLD11* show exons with black rectangles. Genomic sequence for GCG repeat region is shown with numbers with plus sign denoting the start and stop position. Blue background color denotes the GCG repeats. (**C**) Survival rates of 141 rice cultivars after chilling treatment at the seedling stage. For box plots, boxes indicate the 25th to 75th percentile, whiskers indicate the full data range, center lines indicate medians, crosses indicate means, and the numbers below boxes indicate sample size (*n*). *P* values are from two-sided unpaired Student's *t* tests for the mean of cultivars with three GCG repeats versus cultivars with more than three repeats. ***$P < 0.001$. Information for different types of GCG repeats in rice cultivars is shown in dataset S2. *Ind*, *indica*; *TeJ*, *temperate japonica*; *TrJ*, *tropical japonica*.

under chilling stress (Fig. 6, A, B, and D). As a control, seedlings were grown under normal temperature, and there were no obvious DSBs in their root tips (fig. S4A). To further confirm the DSB repair ability in different rice accessions, representative varieties with different GCG repeats in *COLD11* were selected for IFA. As result, more severe DSBs were observed in accessions with three GCG repeats compared with accessions with more than three GCG repeats after chilling treatment (Fig. 6, A and C). Seedlings grown under normal temperature show no obvious DSBs in root tips (fig. S4B). These results indicated that the *COLD11* with more than three GCG repeats have higher DSB repair ability. To confirm the subcellular localization of COLD11, $COLD11^{GLA4}$-*GFP* and $COLD11^{W1943}$-*GFP* were transformed into rice protoplasts with the nuclear marker histone 2B–red fluorescent protein (H2B-RFP). COLD11 was visible as punctate foci in the nucleus (Fig. 7A). RAD51 paralogs function as a complex during DSB repair in mammalian cells and *Arabidopsis* (*22*, *27*), but its functional mechanism is unclear in rice. Bimolecular fluorescence complementation (BiFC) and coimmunoprecipitation (co-IP) assays were performed to explore whether COLD11 forms a dimer or functions alone when binding to DNA. Our results indicated that COLD11 formed a dimer when exerting its function under chilling stress (Fig. 7, B and C). The N-terminal domain of RAD51 affects its interaction with other proteins (*28*–*30*), and GCG repeats are located at the N terminus of *COLD11*. To evaluate the effect of GCG repeats on dimer formation, the mutant genotype of $COLD11^{\Delta GCG}$ was constructed by deleting all the GCG repeats in $COLD11^{GLA4}$ (fig. S2A). Yeast two-hybrid assay was performed with $COLD11^{\Delta GCG}$, $COLD11^{GLA4}$ (3 GCG), and $COLD11^{W1943}$ (10 GCG), and the comparison was carried out by adjusting the initial concentration of yeast cell to be consistent. We found that the interaction ability of $COLD11^{\Delta GCG}$ was notably stronger than that of $COLD11^{GLA4}$ and $COLD11^{W1943}$, indicating that GCG repeats have a clear effect on dimer formation (Fig. 7D).

To clarify whether manipulating *COLD11* affects agronomic traits under normal temperature, we investigated 1000-grain weights, effective tillering numbers, seed number per panicle, and setting rates for CSSL11-1. The results showed that the introduction of $COLD11^{W1943}$ had no negative effects on agronomic traits such as grain yield, compared with its parent line GLA4 (fig. S4, D to H). These results suggested the great potential of $COLD11^{W1943}$ in improving rice chilling tolerance.

DISCUSSION

There are two strategies used by plants to tolerate chilling, defense and repair. Once chilling occurs, cold signals are sensed by sensor complexes, such as COLD1/RGA, and trigger downstream stress response mediated by calcium or other signals (*7*). There are various downstream defense responses including the acceleration of metabolism pathways such as trehalose synthesis (*9*), which provides enough osmotic substances to maintain osmotic potential at low temperature. Despite these precautions, there is still a possibility of DNA damage induced by chilling stress (*23*). Plants must repair this damage in a timely manner to ensure survival. The major QTL gene *COLD11* is a typical example of a gene responsible for DNA repair and is also a potential gene that can be used in molecular design breeding. COLD11 contributes to the repair of DSBs

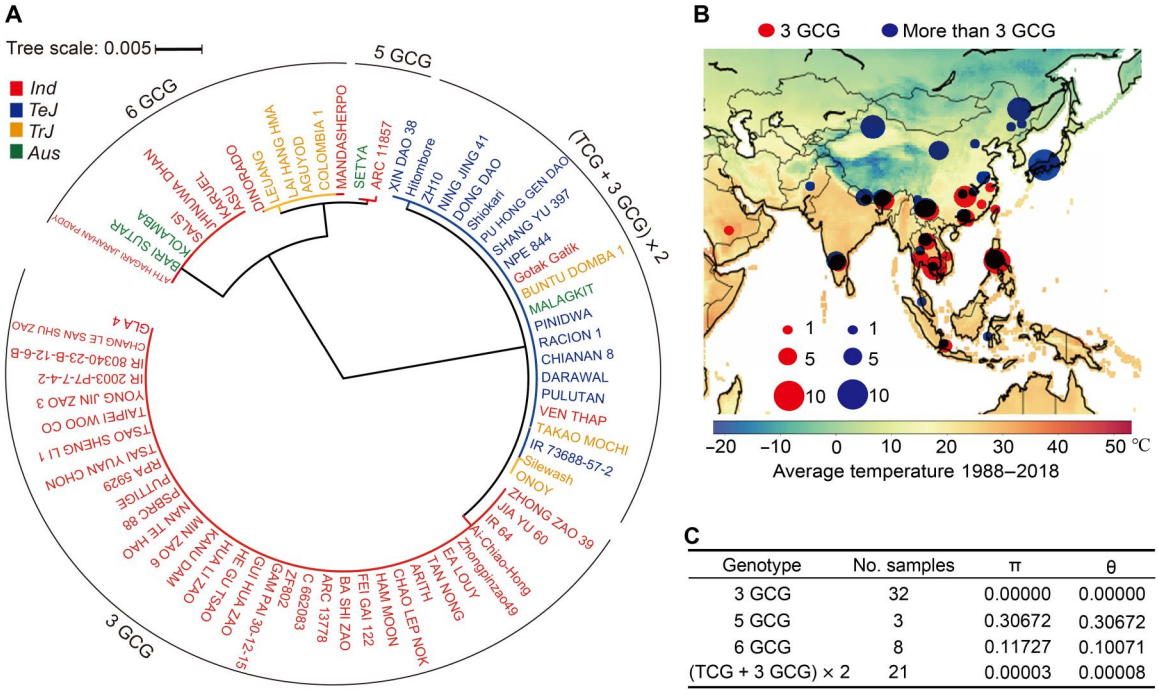

Genotype	No. samples	π	θ
3 GCG	32	0.00000	0.00000
5 GCG	3	0.30672	0.30672
6 GCG	8	0.11727	0.10071
(TCG + 3 GCG) × 2	21	0.00003	0.00008

Fig. 5. Phylogenetic, population genetic, and geographic analysis of *COLD11*. (**A**) Phylogenetic tree for *COLD11*. The phylogenetic tree was generated with the genome sequences of *COLD11* from 43 *indica*, 15 temperate *japonica*, 8 tropical *japonica*, and 4 *Aus* varieties. (**B**) Geographic distribution of rice cultivars based on different types of GCG repeats in *COLD11*. Red and blue dots represent the rice cultivars with the first exon of *COLD11* containing three GCG repeats and more than three repeats, respectively. Geographic distribution of rice varieties is indicated in the map. The color indicates the terrestrial surface temperatures (°C) averaged from 1988 to 2018 (National Centers for Environmental Information; www.ncdc.noaa.gov/) (*41*). (**C**) Nucleotide polymorphism and neutrality tests of *COLD11*. π indicates the average number of pairwise nucleotide differences per site. θ indicates Watterson's estimator of θ per base pair. In (A) and (C), 3 GCG, 5 GCG, 6 GCG, and (TCG + 3 GCG) × 2 represent different types of *COLD11* alleles based on GCG repeats in the first exon: three GCG, five GCG, six GCG, and two copies of TCG + 3 GCG, respectively.

in plants, which can obtain a timely remedy after suffering from chilling damage. It may be the last line of defense for cell survival under chilling stress, in addition to the physiological defense responses induced by cold signaling, such as osmotic adjustment.

COLD11 was identified as a major QTL gene for chilling tolerance through data-merging GWAS of *japonica* and *indica*, two rice subspecies with substantial divergence in chilling tolerance. A key regulatory site was identified in the first exon of *COLD11*. Rice varieties with more GCG codon repeats have higher DSB repair ability and chilling tolerance. Phylogenetic and geographic distribution analysis confirmed the contribution of these repeats to chilling tolerance. GCG encodes alanine and is located at the N terminus of COLD11. The N terminus of RAD51 has been shown to contribute to protein interactions, such as the BRCA2-RAD51 interaction, which facilitates nucleoprotein filament formation on ssDNA generated at the site of DNA damage (*28*, *30*). Our results showed that COLD11 could form dimers, and the GCG repeats at the N terminus affect dimer formation (Fig. 7D), thus affecting the DNA repair ability in the process of chilling response. The discovery of this key site in *COLD11* opens the way for fine regulation of rice chilling tolerance with a single site.

MATERIALS AND METHODS

Plant materials

A total of 464 rice cultivars, collected from different countries around the world, were used for GWASs. CSSLs with a segment containing genes from NIP—namely, CSSL1-1, CSSL1-2, CSSL3-1, CSSL5-1, and CSSL7-1—were developed by crossing NIP with 93-11 and backcrossing with 93-11 at least six times. CSSL11-1 and CSSL11-3, which contains the *COLD11* gene from *O. rufipogon* W1943, *japonica* NIP, were developed by crossing W1943 and NIP with GLA4 independently and backcrossing F_1 with GLA4 at least six times; hybrid plants were selected during every generation for backcrossing. CSSL11-2, which carries the *COLD11* gene from SYN, was developed by crossing SYN and HJX74 and backcrossing F_1 with HJX74 at least six times. For fine mapping of the *COLD11* gene, CSSL11-1 was hybridized with GLA4 and self-pollinated to generate BC_7F_2 plants.

The *cold11* mutants were obtained using the CRISPR-Cas9 system (*31*). A 20-nucleotide guide sequence was selected as the target sequence with E-CRISP tools (www.e-crisp.org/E-CRISP/index.html). Oligonucleotides containing the target sequence were synthesized and then annealed in vitro in a thermocycler. Annealed oligonucleotides were ligated into a CRISPR-Cas9 vector (*31*) and digested with Bsa I. The resulting construct was transformed into CSSL11-1 or GLA4 to generate *cold11* mutants using the *Agrobacterium*-mediated transformation method as previously reported (*32*). For the complementation line, the full-length complementary DNA (cDNA) of $COLD11^{W1943}$ was amplified and ligated into the pUN1301 vector driven by a *Ubiquitin* promoter, and the resulting construct was transformed into the *cold11-1* mutant via *Agrobacterium*-mediated transformation (*32*).

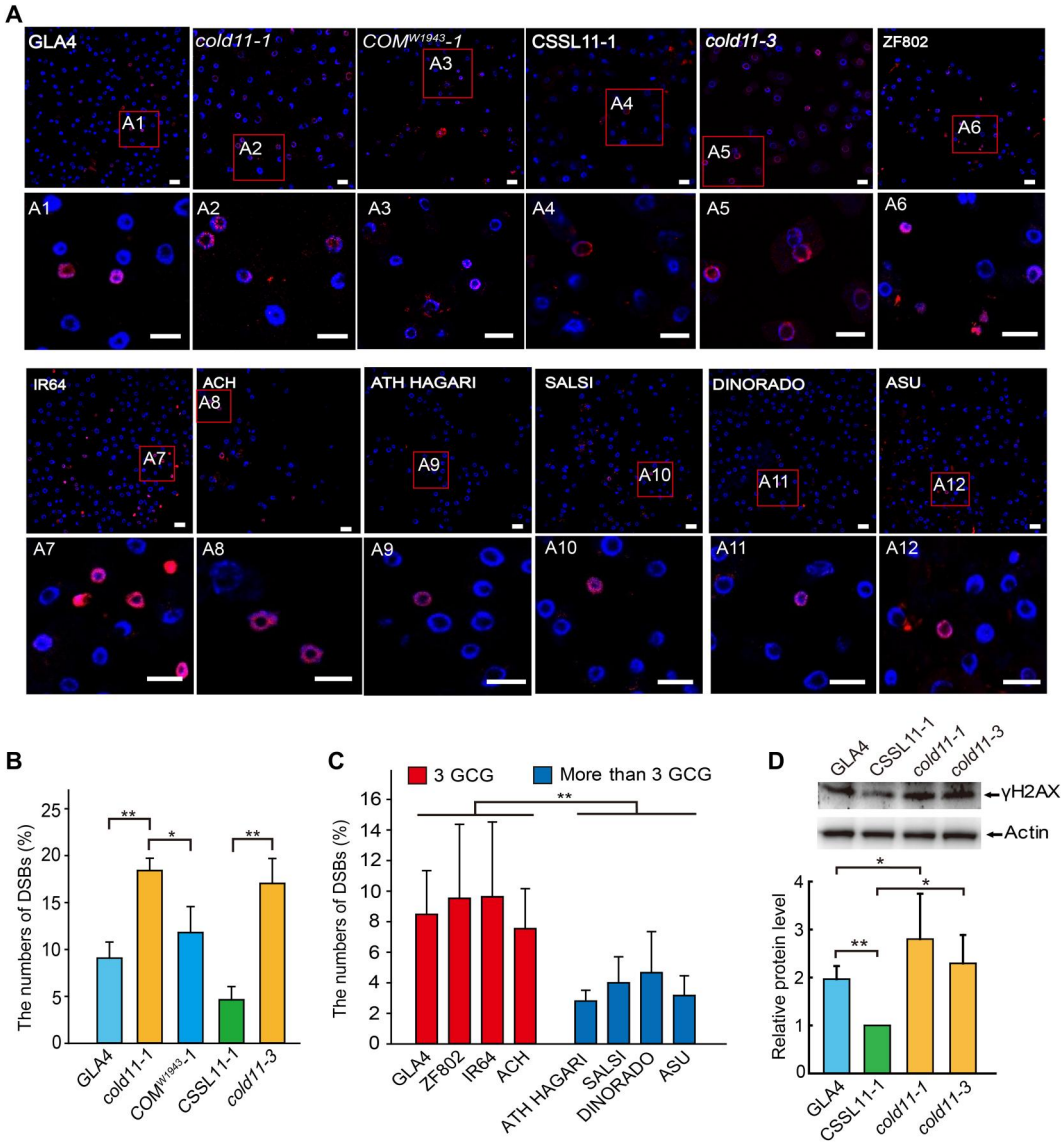

Fig. 6. *COLD11* regulation of chilling tolerance relies upon its DSB repair ability. (**A**) IFA to detect DSBs in the root tips of *COLD11* knockout mutant *cold11-1*, wild-type control GLA4 and the complementation line *COM*^{W1943}*-1*, knockout mutant *cold11-3* and its control CSSL11-1, and rice accessions with *COLD11* containing three GCG repeats and more than three GCG repeats after chilling stress. The bottom images with labels A1 to A12 are enlargements of the regions framed in red in the top images. Three technical experiments were performed with representative images shown. Scale bars, 10 μm. (**B**) Quantification of DSBs in plants exemplified in (A). The number of DSBs was quantified by dividing the cells that produced DSBs by all the cells. Three technical experiments were performed. (**C**) Quantification of DSBs in plants exemplified in (A). The number of DSBs was quantified by dividing the cells that produced DSBs by all the cells. Analyses were performed in three technical replicates. (**D**) Analysis of DNA damage by Western blot analysis with γH2AX antibody in the root tip cells of *COLD11* knockout mutant *cold11-1* and *cold11-3*, as well as wild-type control GLA4 and CSSL11-1, after chilling stress, with actin serving as the loading control (top). Protein intensity was quantified with ImageJ. Protein level in CSSL11-1 was set as "1" (bottom). Values in (B) to (D) are shown as means ± SD (n = 3); P values were generated using Student's t test; *P < 0.05 and **P < 0.01.

Chilling treatment and tolerance analysis

Chilling treatment was carried out as reported previously (*9*) with minor modifications. All samples were grown in 96-well plates with Kimura B nutrient solution in a greenhouse with a 28°/25°C day/night temperature. Seedlings at the three-leaf stage were subjected to chilling treatment at 4° ± 0.5°C for various times. For GWAS, *japonica* varieties were subjected to chilling treatment for 60 hours, and *indica* varieties were treated for 30 hours. For chilling tolerance analysis of 141 cultivars, *indica* varieties were subjected to chilling treatment for 30 hours, temperate *japonica* varieties were treated for 60 hours, and tropical *japonica* varieties were treated for 48 hours. For chilling tolerance analysis of CSSLs, materials with the CSSL11-1 background were subjected to chilling treatment for 32 hours, CSSLs with the 93-11 background were treated for 40 hours, and materials with the CSSL11-2 background were treated for 48 hours. After treatment, seedlings were transferred back to the greenhouse and grown for 14 days for recovery. Survival rates are shown as the percentage of surviving seedlings versus the total

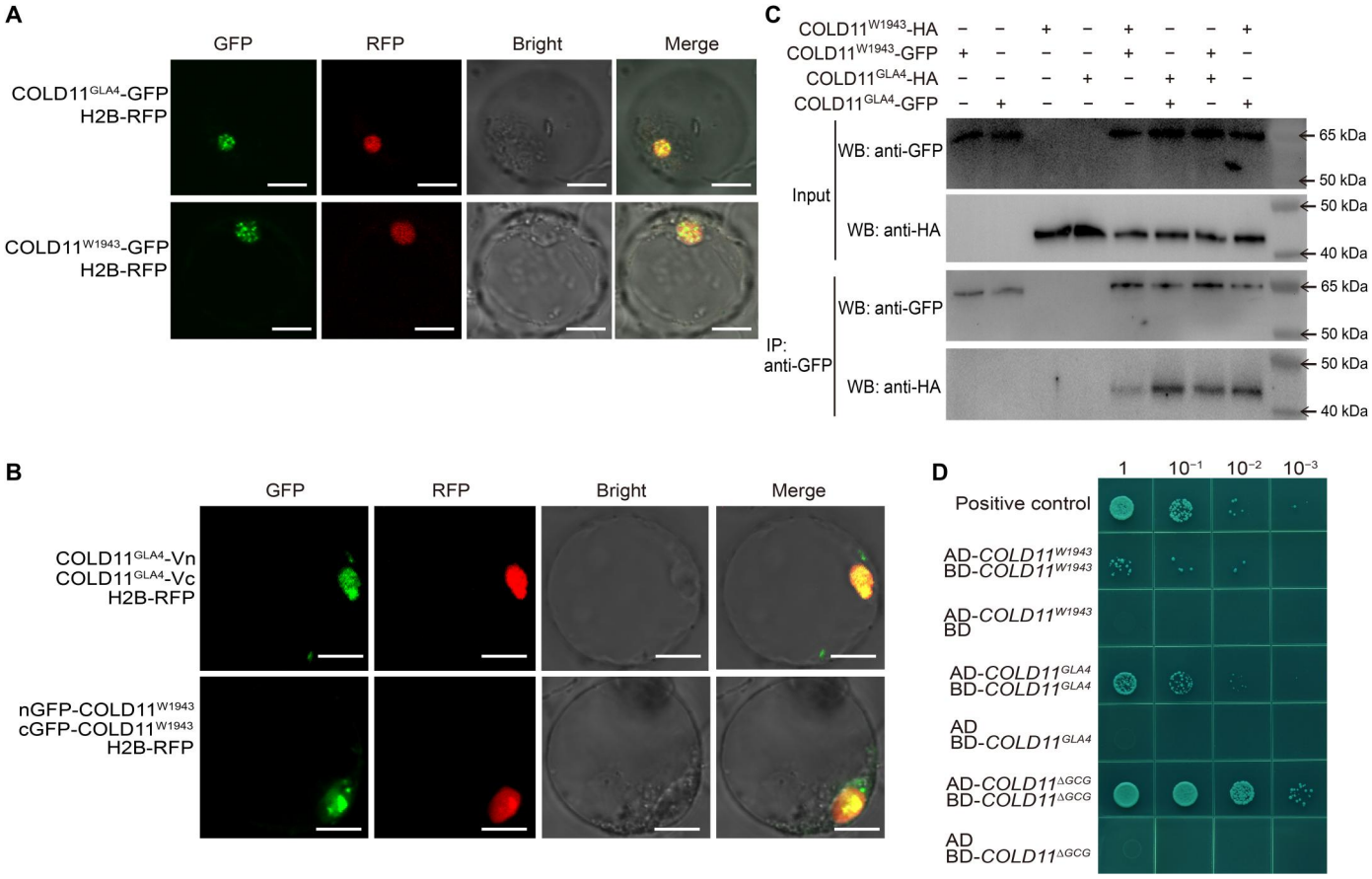

Fig. 7. Subcellular localization and dimer formation analysis for COLD11. (**A**) Subcellular localization of COLD11^{GLA4} and COLD11^{W1943} in rice protoplasts. COLD11^{GLA4}-GFP and COLD11^{W1943}-GFP signals were merged with that of the RFP-tagged H2B marker. Scale bars, 10 μm. (**B**) BiFC assays of rice protoplasts demonstrating dimer formation for COLD11. H2B-RFP was used as the protein marker. Scale bars, 10 μm. (**C**) Co-IP assay demonstrating dimer formation for COLD11. Proteins extracted from rice protoplasts with (+) or without (−) HA-tagged COLD11^{W1943} and COLD11^{GLA4} or GFP-tagged COLD11^{W1943} and COLD11^{GLA4} were incubated with agarose beads and anti-GFP antibody. Input and IP samples were immunoblotted with anti-GFP and anti-HA antibodies. (**D**) Yeast two-hybrid assays demonstrating dimer formation for COLD11. The combination of AD-OsbHLH002 and BD-OsMAPK3 was used as a positive control. Yeasts were gradient diluted as 1, 10^{-1}, 10^{-2}, and 10^{-3}. WB, Western blot.

number of tested plants. The experiments were performed independently at least three times.

Statistical analysis

All 464 rice cultivars were genotyped by genome resequencing, and 5,108,184 SNPs were identified. We implemented data quality control by excluding the SNPs with a missing rate of >20%, minimal count of three genotypes of <5, and minor allele frequency of <5%. In total, 2,134,700 SNPs passed the filters. To adjust for population stratification, we performed principal components analysis on 20,000 SNPs that were distributed evenly on 12 chromosomes (*33*, *34*) and chose the top 10 principal components with the Tracy-Widom statistic for the eigenvalues greater than 2.0234 as covariates in the association tests.

We used the MDS approach to combine two datasets: survival rates of rice cultivars at 30 and 60 hours. The MDS technique is commonly used for dimensionality reduction, and it is capable of discovering a low-dimensional embedding of the high-dimensional data points that preserves their interpoint distances (*35*). Let $\boldsymbol{Y}$ be the data matrix of n subjects for m outcomes (here, $n = 464$, $m = 2$). We centralized $\boldsymbol{Y}$ by subtracting the column means and dividing by the column SD, that is, $\boldsymbol{Y_c}=\mathbf{HY}$, where $\mathbf{H} = \mathbf{I}_n - \mathbf{1}_n\mathbf{1}_n^{\tau}/n$, $\mathbf{I}_n$ is an n-dimensional identity matrix, $\mathbf{1}_n$ is a vector of length n with all elements being 1, and τ denotes the transpose of a vector or a matrix. The eigenvalues of $\boldsymbol{Y_c}\boldsymbol{Y_c}^{\tau}$ are denoted by $\lambda_1 \geq ... \geq \lambda_m$ and the corresponding eigenvectors by $\upsilon_1, ..., \upsilon_m$. The MDS outcomes are given by $Z_j = \upsilon_j/\sqrt{\lambda_j}, j = 1, ..., k$, where k is determined by

$$k = \underset{j}{\operatorname{argmin}}\left\{ j \mid \frac{\lambda_1 + \lambda_2 + \ldots + \lambda_j}{\lambda_1 + \lambda_2 + \ldots + \lambda_m} \geq 0.85, j = 1, 2, \ldots, m \right\}$$

For the current survival rate data, k is equal to 1. It can be seen from Fig. 1A that the MDS outcome tends to be more informative than a single outcome when separating the two subspecies of Asian cultivated rice: *japonica* and *indica*.

We used the BF for the linear regression model to evaluate the evidence of association between the combined outcome and SNPs (*11*, *12*, *36*). Let H_0 be the null hypothesis of no association and H_1 be the alternative hypothesis. The BF of H_1 versus H_0 is defined as

$$\mathrm{BF}_{10} = \frac{\Pr(\mathrm{Data} \mid H_1)}{\Pr(\mathrm{Data} \mid H_0)} = \frac{\int \Pr(\mathrm{Data} \mid \theta_1, H_1)\Pr(\theta_1 \mid H_1)d\theta_1}{\int \Pr(\mathrm{Data} \mid \theta_0, H_0)\Pr(\theta_0 \mid H_0)d\theta_0}$$

where θ_0 and θ_1 are the parameters for the null and alternative hypothesis, respectively. BF_{10} quantifies how much more likely the data are under H_1 than H_0. We used the R package "bain" with the same prior for the parameters $Pr(\theta_i \mid H_i)$, $i = 0,1$, to calculate the BFs, where the prior of θ_0 is the standard normal distribution. The thresholds of association magnitude for BFs followed those by Kass and Raftery (*37*), where, when BF > 3, 20, and 150, the evidence is positive, strong, and very strong in favor of H_1, respectively. Pearson correlation coefficient was used to measure the linear relationship between the SNPs of candidate interval and the survival rates from 123 representative accessions.

The Pearson correlation coefficient is the correlation between the interaction profiles of "A" and "B" (*17*). Let genotype be A and survival rates be B; the Pearson correlation coefficient and significance test are generated with IBM SPSS Statistics (https://spss.en.softonic.com/), and detailed information is listed in dataset S4.

Quantitative RT-PCR

Total RNA was extracted from rice tissues using the RNA Simple Total RNA Kit (TIANGEN, China) according to the manufacturer's instructions. The RNA samples were reverse-transcribed using the one-step gDNA Removal and cDNA Synthesis Kit (TransGen Biotech, China). Quantitative real-time polymerase chain reaction (qRT-PCR) was performed with SYBR Green PCR Master Mix (Thermo Fisher Scientific, Waltham, MA, USA) according to the manufacturer's protocol in an Mx3000P Real-Time PCR System (Stratagene, USA). The *18sRNA* or *Ubiquitin* gene was used as the reference. Analyses were performed in three biological replicates. The primers used in qRT-PCR are listed in dataset S3.

Coimmunoprecipitation

The co-IP assay was carried out to clarify whether COLD11 could form a dimer. $COLD11^{W1943}$ and $COLD11^{GLA4}$ were ligated into the pBI221 [35S::GFP (green fluorescent protein)] and modified pBI221 [35S::HA (hemagglutinin)] vectors to generate 35S::$COLD11^{W1943}$-HA, 35S::$COLD11^{GLA4}$-HA, 35S::$COLD11^{W1943}$-GFP, and 35S::$COLD11^{GLA4}$-GFP plasmids, respectively. 35S::$COLD11^{W1943}$-HA + 35S::$COLD11^{W1943}$-GFP, 35S::$COLD11^{GLA4}$-HA + 35 s::$COLD11^{GLA4}$-GFP, 35S::$COLD11^{W1943}$-HA + 35 s::$COLD11^{GLA4}$-GFP, and 35S::$COLD11^{GLA4}$-HA + 35S::$COLD11^{W1943}$-GFP were transformed into rice protoplasts. Total proteins from rice protoplasts were incubated with agarose beads and anti-GFP antibody (ABclonal). The immunoprecipitated proteins were detected with anti-GFP (ABclonal) and anti-HA (ABclonal) antibody.

Yeast two-hybrid assay

The full-length cDNA of $COLD11^{W1943}$, $COLD11^{GLA4}$, and deletion GCG repeat $COLD11^{\Delta GCG}$ (fig. S2A) were amplified and ligated into the pGADT7 and pGBKT7 vectors to generate pGADT7-$COLD11^{W1943}$, pGBKT7-$COLD11^{W1943}$, pGADT7-$COLD11^{GLA4}$, pGBKT7-$COLD11^{GLA4}$, pGADT7-$COLD11^{\Delta GCG}$, and pGBKT7-$COLD11^{\Delta GCG}$. pGADT7-$COLD11^{W1943}$ + pGBKT7-$COLD11^{W1943}$, pGADT7-$COLD11^{GLA4}$ + pGBKT7-$COLD11^{GLA4}$, and pGADT7-$COLD11^{\Delta GCG}$ + pGBKT7-$COLD11^{\Delta GCG}$ were transformed into *Saccharomyces cerevisiae* strain EGY48. The transformed yeast cells were grown on synthetically defined medium (SD medium) lacking Leu and Trp (SD/-Leu-Trp) at 30°C for 2 days, then yeast cells were suspended into sterility solution to adjust its concentration, and the initial concentration is adjusted to optical density at 600 nm = 1 and then diluted 10^{-1}, 10^{-2}, and 10^{-3}. The adjusted yeast cells were transferred to SD/-Trp/-Leu/-His/-Ade containing X-α-Gal (5-bromo-4-chloro-3-indolyl-α-D-galactoside) for blue color development. The combination of AD-OsbHLH002 and BD-OsMAPK3 was used as a positive control (*9*). The plasmids pGADT7 and pGBKT7 were used as negative controls. Primers used for the yeast two-hybrid assays are listed in dataset S3.

Immunofluorescence staining analysis

We used hydroponically grown seedling roots of CSSL11-1, GLA4, the *cold11* mutants, and the complementation line for immunofluorescence staining analysis. After chilling treatment, root tips were collected and fixed in 4% paraformaldehyde solution at 24°C for 45 min and then enzymatically degraded by 2% cellulose and 1% pectinase. Root tip cells were fixed on a slide, and then, the slide was incubated with the γH2AX antibody at 37°C for 1 hour. Goat anti-rabbit immunoglobulin (Ig; SouthernBiotech, USA) was added to the slide in darkness and then incubated at 37°C for 40 min. The γH2AX antibody was obtained according to methods from previous reports (*38*). The nuclei were stained with Antifade Mounting Medium containing 4′,6-diamidino-2-phenylindole (Beyotime, P0131), and the immunofluorescence signals were captured with a fluorescence microscope (Leica TCS SP5). We randomly chose samples with chilling treatment for photographic and quantitative analysis. Analyses were performed in three biological replicates, and at least 10 plants were analyzed for each sample.

Western blot analysis

Proteins extracted from root tip cells were used for Western blot analysis. Proteins were fractionated by SDS–polyacrylamide gel electrophoresis on a 12% tris/glycine SDS precast polyacrylamide gel (Bio-Rad, USA) and subjected to immunoblotting using Super-Signal West Dura maximum sensitivity substrate (Thermo Fisher Scientific, USA) according to the manufacturer's protocol. Polyclonal antibody γH2AX and rabbit anti-goat IgG (Origene, USA) were used for immunoblotting. Actin was used as the internal reference protein.

Phylogenetic analysis

The full length of *COLD11* in different plant materials was sequenced for haplotype and phylogenetic analysis. The primer sequences are listed in dataset S3. The gene sequences of 70 accessions (43 *indica*, 15 temperate *japonica*, 8 tropical *japonica*, and 4 *Aus*) were obtained. The neighbor-joining method in MEGA 6.0 was used for constructing the phylogenetic tree (*18*).

Grain yield evaluation

Grain yield measurement was carried out as reported previously (*7*). GLA4 and CSSL11-1 were grown in the greenhouse under a short-day photoperiod (10-hour day/14-hour night) with a light strength of 1.35× 10,000 lux and temperature of 30°/25°C (day/night). GLA4 and CSSL11-1 were grown together to ensure that the experimental conditions were the same until the mature stage. More than 10 plants were randomly chosen to investigate tiller number per plant. Similarly, more than 10 panicles from different plants were randomly chosen and used to evaluate the number of seeds per panicle. One thousand seeds per sample from different plants were randomly chosen and measured for 1000-grain weight. All

experiments were replicated at least three times. Student's *t* test was used to generate the *P* values.

Subcellular localization and BiFC assays

To determine the subcellular localization of COLD11, two transient expression vectors, *35S::COLD11*^{GLA4}*-GFP* and *35S::COLD11*^{W1943}*-GFP*, were constructed. The protoplasts were incubated at 25°C for 18 hours after transformation and then observed under a fluorescence microscope (Leica TCS SP5). For BiFC assays, the coding sequences of *COLD11*^{GLA4} and *COLD11*^{W1943} were amplified. *COLD11*^{GLA4} was infused as *35S::COLD11*^{GLA4}*-Vn* and *35S::COLD11*^{GLA4}-Vc, while *COLD11*^{W1943} was infused as *35S::nGFP-COLD11*^{W1943} and *35S::cGFP-COLD11*^{W1943} (*39*). The vectors were transformed into rice protoplasts, obtained from leaf sheaths and stalks of 10-day-old etiolated rice seedlings, via the polyethylene glycol 4000 method (*40*). The *35S::H2B-RFP* was co-transformed into the protoplast cells as a marker protein. The transformed protoplasts were observed under a fluorescence microscope (Leica TCS SP5), and the pictures were analyzed using Image LAS-AF-Lite_2.6.0 (www.leica-microsystems.com/).

FDA/PI staining

We used hydroponically grown seedlings of CSSL11-1, GLA4, the *cold11* mutants, and the complementation line for FDA/PI staining analysis (*16*). After incubation under normal temperature conditions (25°/28°C, night/day) or chilling conditions (GLA4, *cold11-1*, and *COM*^{W1943}*-1* were incubated at 4°C for 28 hours; CSSL11-1 and *cold11-3* were incubated at 4°C for 32 hours), parenchyma cells were collected into 1× phosphate-buffered saline solution and stained with 5 μM FDA and 10 μM PI for 30 min in darkness. The stained cells were observed under a fluorescence microscope (Leica TCS SP5), and the pictures were analyzed using Image LAS-AF-Lite_2.6.0 (www.leica-microsystems.com/) and ImageJ software (https://imagej.nih.gov/ij/download.html).

Supplementary Materials

This PDF file includes:
Figs. S1 to S4

Other Supplementary Material for this manuscript includes the following:
Datasets S1 to S4

REFERENCES AND NOTES

1. T. Zhang, E. Guo, Y. Shi, C. Xue, X. Zhu, X. Dong, T. Li, L. Wang, S. Jiang, H. Xiang, L. Wang, Y. Feng, Y. Lai, T. Cao, S. Li, S. Ma, H. Ma, L. Zhou, X. Wang, X. Yang, Modelling the advancement of chilling tolerance breeding in Northeast China. *J. Agro. Crop Sci.* **207**, 984–994 (2021).
2. R. P. da Cruz, R. A. Sperotto, D. Cargnelutti, J. M. Adamski, T. de Freitas Terra, J. P. Fett, Avoiding damage and achieving cold tolerance in rice plants. *Food Energy Secur.* **2**, 96–119 (2013).
3. Y. Lv, Z. Guo, X. Li, H. Ye, X. Li, L. Xiong, New insights into the genetic basis of natural chilling and cold shock tolerance in rice by genome-wide association analysis. *Plant Cell Environ.* **39**, 556–570 (2016).
4. C. Liu, S. Ou, B. Mao, J. Tang, W. Wang, H. Wang, S. Cao, M. R. Schlappi, B. Zhao, G. Xiao, X. Wang, C. Chu, Early selection of *bZIP73* facilitated adaptation of *japonica* rice to cold climates. *Nat. Commun.* **9**, 3302 (2018).
5. V. C. Andaya, D. J. Mackill, Mapping of QTLs associated with cold tolerance during the vegetative stage in rice. *J. Exp. Bot.* **54**, 2579–2585 (2003).
6. J. Zhang, X. M. Li, H. X. Lin, K. Chong, Crop improvement through temperature resilience. *Annu. Rev. Plant Biol.* **70**, 753–780 (2019).
7. Y. Ma, X. Dai, Y. Xu, W. Luo, X. Zheng, D. Zeng, Y. Pan, X. Lin, H. Liu, D. Zhang, J. Xiao, X. Guo, S. Xu, Y. Niu, J. Jin, H. Zhang, X. Xu, L. Li, W. Wang, Q. Qian, S. Ge, K. Chong, *COLD1* confers chilling tolerance in rice. *Cell* **160**, 1209–1221 (2015).
8. Z. Zhang, J. Li, Y. Pan, J. Li, L. Zhou, H. Shi, Y. Zeng, H. Guo, S. Yang, W. Zheng, J. Yu, X. Sun, G. Li, Y. Ding, L. Ma, S. Shen, L. Dai, H. Zhang, S. Yang, Y. Guo, Z. Li, Natural variation in *CTB4a* enhances rice adaptation to cold habitats. *Nat. Commun.* **8**, 14788 (2017).
9. Z. Zhang, J. Li, F. Li, H. Liu, W. Yang, K. Chong, Y. Xu, OsMAPK3 phosphorylates OsbHLH002/OsICE1 and inhibits its ubiquitination to activate *OsTPP1* and enhances rice chilling tolerance. *Dev. Cell* **43**, 731–743.e5 (2017).
10. X. Guo, D. Liu, K. Chong, Cold signaling in plants: Insights into mechanisms and regulation. *J. Integr. Plant Biol.* **60**, 745–756 (2018).
11. The Wellcome Trust Case Control Consortium, Genome-wide association study of 14,000 cases of seven common diseases and 3,000 shared controls. *Nature* **447**, 661–678 (2007).
12. M. Stephens, D. J. Balding, Bayesian statistical methods for genetic association studies. *Nat. Rev. Genet.* **10**, 681–690 (2009).
13. D. Mao, C. Chen, Colinearity and similar expression pattern of rice *DREB1s* reveal their functional conservation in the cold-responsive pathway. *PLOS ONE* **7**, e47275 (2012).
14. D. D. Figueiredo, P. M. Barros, A. M. Cordeiro, T. S. Serra, T. Lourenco, S. Chander, M. M. Oliveira, N. J. Saibo, Seven zinc-finger transcription factors are novel regulators of the stress responsive gene *OsDREB1B*. *J. Exp. Bot.* **63**, 3643–3656 (2012).
15. J. Xu, Q. Zhao, P. Du, C. Xu, B. Wang, Q. Feng, Q. Liu, S. Tang, M. Gu, B. Han, G. Liang, Developing high throughput genotyped chromosome segment substitution lines based on population whole-genome re-sequencing in rice (*Oryza sativa* L.). *BMC Genomics* **11**, 656 (2010).
16. K. Jones, D. W. Kim, J. S. Park, C. H. Khang, Live-cell fluorescence imaging to investigate the dynamics of plant cell death during infection by the rice blast fungus *Magnaporthe oryzae*. *BMC Plant Biol.* **16**, 69 (2016).
17. J. I. F. Bass, A. Diallo, J. Nelson, J. M. Soto, C. L. Myers, A. J. Walhout, Using networks to measure similarity between genes: Association index selection. *Nat. Methods* **10**, 1169–1176 (2013).
18. K. Tamura, G. Stecher, D. Peterson, A. Filipski, S. Kumar, MEGA6: Molecular evolutionary genetics analysis version 6.0. *Mol. Biol. Evol.* **30**, 2725–2729 (2013).
19. B. L. Mahaney, K. Meek, S. P. Lees-Miller, Repair of ionizing radiation-induced DNA double-strand breaks by non-homologous end-joining. *Biochem. J.* **417**, 639–650 (2009).
20. W. P. Roos, B. Kaina, DNA damage-induced cell death by apoptosis. *Trends Mol. Med.* **12**, 440–450 (2006).
21. D. Tang, C. Miao, Y. Li, H. Wang, X. Liu, H. Yu, Z. Cheng, OsRAD51C is essential for double-strand break repair in rice meiosis. *Front. Plant Sci.* **5**, 167 (2014).
22. H. Yokoyama, N. Sarai, W. Kagawa, R. Enomoto, T. Shibata, H. Kurumizaka, S. Yokoyama, Preferential binding to branched DNA strands and strand-annealing activity of the human Rad51B, Rad51C, Rad51D and Xrcc2 protein complex. *Nucleic Acids Res.* **32**, 2556–2565 (2004).
23. J. H. Hong, M. Savina, J. Du, A. Devendran, K. Kannivadi Ramakanth, X. Tian, W. S. Sim, V. V. Mironova, J. Xu, A sacrifice-for-survival mechanism protects root stem cell niche from chilling stress. *Cell* **170**, 102–113.e14 (2017).
24. Y. Morozumi, R. Ino, S. Ikawa, N. Mimida, T. Shimizu, S. Toki, H. Ichikawa, T. Shibata, H. Kurumizaka, Homologous pairing activities of two rice RAD51 proteins, RAD51A1 and RAD51A2. *PLOS ONE* **8**, e75451 (2013).
25. C. Rajanikant, M. Melzer, B. J. Rao, J. K. Sainis, Homologous recombination properties of OsRad51, a recombinase from rice. *Plant Mol. Biol.* **68**, 479–491 (2008).
26. R. B. Jensen, A. Carreira, S. C. Kowalczykowski, Purified human BRCA2 stimulates RAD51-mediated recombination. *Nature* **467**, 678–683 (2010).
27. H. Su, Z. Cheng, J. Huang, J. Lin, G. P. Copenhaver, H. Ma, Y. Wang, *Arabidopsis* RAD51, RAD51C and XRCC3 proteins form a complex and facilitate RAD51 localization on chromosomes for meiotic recombination. *PLOS Genet.* **13**, e1006827 (2017).
28. S. Subramanyam, W. T. Jones, M. Spies, M. A. Spies, Contributions of the RAD51 N-terminal domain to BRCA2-RAD51 interaction. *Nucleic Acids Res.* **41**, 9020–9032 (2013).
29. V. E. Galkin, Y. Wu, X. P. Zhang, X. Qian, Y. He, X. Yu, W. D. Heyer, Y. Luo, E. H. Egelman, The Rad51/RadA N-terminal domain activates nucleoprotein filament ATPase activity. *Structure* **14**, 983–992 (2006).
30. V. E. Galkin, F. Esashi, X. Yu, S. X. Yang, S. C. West, E. H. Egelman, BRCA2 BRC motifs bind RAD51-DNA filaments. *Proc. Natl. Acad. Sci. U.S.A.* **102**, 8537–8542 (2005).
31. X. Ma, Q. Zhang, Q. Zhu, W. Liu, Y. Chen, R. Qiu, B. Wang, Z. Yang, H. Li, Y. Lin, Y. Xie, R. Shen, S. Chen, Z. Wang, Y. Chen, J. Guo, L. Chen, X. Zhao, Z. Dong, Y. G. Liu, A robust CRISPR/Cas9 system for convenient, high-efficiency multiplex genome editing in monocot and dicot plants. *Mol. Plant* **8**, 1274–1284 (2015).

32. Q. Ma, X. Dai, Y. Xu, J. Guo, Y. Liu, N. Chen, J. Xiao, D. Zhang, Z. Xu, X. Zhang, K. Chong, Enhanced tolerance to chilling stress in *OsMYB3R-2* transgenic rice is mediated by alteration in cell cycle and ectopic expression of stress genes. *Plant Physiol.* **150**, 244–256 (2009).
33. A. L. Price, N. J. Patterson, R. M. Plenge, M. E. Weinblatt, N. A. Shadick, D. Reich, Principal components analysis corrects for stratification in genome-wide association studies. *Nat. Genet.* **38**, 904–909 (2006).
34. Q. Li, K. Yu, Improved correction for population stratification in genome-wide association studies by identifying hidden population structures. *Genet. Epidemiol.* **32**, 215–226 (2008).
35. J. B. Tenenbaum, V. de Silva, J. C. Langford, A global geometric framework for nonlinear dimensionality reduction. *Science* **290**, 2319–2323 (2000).
36. J. Marchini, B. Howie, S. Myers, G. McVean, P. Donnelly, A new multipoint method for genome-wide association studies by imputation of genotypes. *Nat. Genet.* **39**, 906–913 (2007).
37. R. E. Kass, A. E. Raftery, Bayes factors. *J. Am. Stat. Assoc.* **90**, 773–795 (1995).
38. C. Miao, D. Tang, H. Zhang, M. Wang, Y. Li, S. Tang, H. Yu, M. Gu, Z. Cheng, Central region component1, a novel synaptonemal complex component, is essential for meiotic recombination initiation in rice. *Plant Cell* **25**, 2998–3009 (2013).
39. M. Walter, C. Chaban, K. Schutze, O. Batistic, K. Weckermann, C. Nake, D. Blazevic, C. Grefen, K. Schumacher, C. Oecking, K. Harter, J. Kudla, Visualization of protein interactions in living plant cells using bimolecular fluorescence complementation. *Plant J.* **40**, 428–438 (2004).
40. R. Bart, M. Chern, C. J. Park, L. Bartley, P. C. Ronald, A novel system for gene silencing using siRNAs in rice leaf and stem-derived protoplasts. *Plant Methods* **2**, 13 (2006).
41. H. Samuelson, L. Gaches, National environmental satellite, data, and information service: providing global observations to understand earth science systems. *Mar. Technol. Soc. J.* **49**, 23–36 (2015).

Acknowledgments: We thank J. Cao (Key Laboratory of Plant Molecular Physiology, CAS) and Q. Meng (Key Laboratory of Plant Molecular Physiology, CAS) for help with data analysis. We thank Q. Qian (China National Rice Research Institute) and D. Zeng (China National Rice Research Institute) for providing plant material. We are grateful to J. Feng (Key Laboratory of Plant Molecular Physiology, CAS) and Y. Gao (Key Laboratory of Plant Molecular Physiology, CAS) for plant material identification. We thank J. Li (Experimental Platforms of Key Laboratory of Plant Molecular Physiology, CAS) for confocal microscopy assistance. **Funding:** This work was supported by the Strategic Priority Research Program of Chinese Academy of Sciences (grant no. XDA24010301) and the Basic Science Center Program (grant no. 31788103). **Author contributions:** K.C. designed the experiments. Q.L. and J.Z. analyzed GWAS data. Z.L. and B.W. performed and analyzed most of the experiments. W.L. performed experiments on phenotyping of GWAS cultivars. Z.X. performed experiments on IFA assays. J.W. and W.Z. assisted with GWAS analysis. Y.N. and Y.X. contributed to the transgene and manuscript preparation, respectively. Z.C. and S.G. contributed to the DNA damage and phylogenetic analysis, respectively. **Competing interests:** The authors declare that they have no competing interests. **Data and materials availability:** All data needed to evaluate the conclusions in the paper are present in the paper and/or the Supplementary Materials.

Submitted 15 April 2022
Accepted 6 December 2022
Published 6 January 2023
10.1126/sciadv.abq5506